*Nano Research* 2015, 8(12): 3922–3933
DOI 10.1007/s12274-015-0893-9
**Research Article**

ISSN 1998-0124
CN 11-5974/O4

# Enhanced destabilization of mismatched DNA using gold nanoparticles offers specificity without compromising sensitivity for nucleic acid analyses

Abootaleb Sedighi[1,†], Vicki Whitehall[2], and Paul C. H. Li[1] (✉)

[1] *Department of Chemistry, Simon Fraser University, Burnaby, BC, V5A 1S6, Canada*
[2] *QIMR Berghofer Medical Research Institute, 300 Herston Rd, Brisbane QLD 4006, Australia*
[†] *Present address: Department of Chemical and Physical Sciences, University of Toronto, Mississauga, ON, L5L1C6, Canada*

**Received:** 20 June 2015
**Revised:** 4 September 2015
**Accepted:** 8 September 2015



**KEYWORDS**
DNA hybridization,
gold nanoparticles,
single nucleotide polymorphism,
specificity,
CD-like NanoBioArray chip

## ABSTRACT

Here, we report a method that uses gold nanoparticles (AuNPs) to enhance the specificity of DNA hybridization without reducing its detection sensitivity. The conventional stringent wash method utilizes high-temperature/low-salt conditions to enhance the specificity of DNA hybridization-based assays. This method creates a destabilizing environment for base pairing that affects specific and nonspecific duplexes. Therefore, specificity is achieved at the expense of signal intensity or sensitivity. However, in the proposed wash method, AuNPs predominantly destabilize nonspecific duplexes, offering specificity without compromising sensitivity. This AuNP wash technique has proven to be effective in detecting single nucleotide polymorphisms (SNPs) in genomic samples even at room temperature in a CD-like NanoBioArray (CD-NBA) chip. This method is also robust with sequence variation and is compatible with multiplex DNA analyses on microarrays. Thus, the AuNP wash method could potentially be useful for improving the accuracy of DNA hybridization results.

## 1 Introduction

Nucleic acid diagnostics is currently the fastest growing segment of the *in vitro* diagnostics market [1]. However, considering the possibility of a future with personalized medicine, these diagnostic techniques must be simple, fast, and, importantly, reliable [2]. DNA hybridization is a promising tool for nucleic acid diagnostics because the method is simple and has high sample-throughput potential [3]. However, hybridization assays are sometimes interfered by nonspecific binding especially when the hybridization is far from the melting temperature of the DNA duplex [4]. These interferences are the main cause of discrepancies in the results of hybridization-based assays [5]. This limitation is aggravated for single nucleotide polymorphism (SNP) analysis in which the mismatched (MM) target strand varies from the perfectly matched (PM) target strand by only a

Address correspondence to paulli@sfu.ca

single base pair. In order to improve assay specificity, DNA hybridization or the subsequent wash step is conventionally conducted at stringent conditions, when high temperature, low ionic strength, or chemically denaturing medium is applied to reduce the non-specific signal [6]. These stringent conditions bring the duplexes near their melting temperatures, where a marginal difference in duplex stability (i.e., PM vs. MM) causes significant variation in their affinities [7]. However, this high-temperature method is not effective when conducted for highly multiplexed analyses, such as DNA microarrays where many thousands of targets, each with its own melting temperature, have to be analyzed simultaneously at a single optimized temperature [8]. Therefore, low specificity with false-positive and false-negative outcomes are obtained for those targets with melting temperatures far from the hybridization temperature [9]. These faults are widely agreed to be the main pitfalls that impact the accuracy of the DNA microarray platform, resulting in a barrier for its adoption in clinical applications [4, 5, 10–12].

Several novel methods for improving specificity have been reported in which special hybridization probes are designed to work at temperatures well below the melting temperatures [3, 5, 13–18]. For instance, when oligonucleotide probes with short lengths are used, the nonspecific binding is thermodynamically less favorable [13–15], leading to improved sensitivity. However, the design of these special probes are usually complicated and the methods are not compatible with multiplex analyses [3].

We have recently developed a microfluidic bioarray technique that uses gold nanoparticles conjugated to DNA targets (i.e., AuNP targets) for specific detection of SNPs [19, 20]. In this technique, no temperature stringency is required, and high specificities in hybridization are achieved by loading the target strands on the surfaces of small citrate-capped gold nanoparticles prior to their hybridization to the oligonucleotide probes immobilized on the surfaces of the microfluidic channel [19, 20]. Kinetic analyses of DNA hybridization using surface plasmon resonance (SPR) spectroscopy has shown that AuNPs enhance dehybridization of MM duplexes to a greater extent than PM duplexes, thus accounting for most of the SNP discrimination power of the AuNP-enabled technique [21]. However, the AuNP targets result in lower hybridization signal intensities than their free target counterparts (Fig. S1 in the Electronic Supplementary Material (ESM)) [19]. Thus, the quest for an effective and simple SNP detection technique without loss in signal continues.

The results of our previous kinetic analyses demonstrated that the influence of AuNPs is predominantly on dehybridization. Therefore, we attempted to develop a method using AuNPs in the washing (dehybridization) step, rather than in the hybridization step. In this method, a buffer solution containing AuNPs (5 nm in diameter) is used to flow over the surface-bound duplexes for removal by washing (Fig. 1). AuNP-enhanced dehybridization is achieved via binding between AuNPs and the thermally induced openings along the DNA duplexes [21]. AuNP–ssDNA interactions stabilize the openings, and thus accelerate their propagation, which in turn accelerate dehybridization and preferentially destabilize the MM duplexes.

## 2 Experimental

### 2.1 Materials

Gold nanoparticles (with citrate and tannic acid) of 5, 10, and 20 nm diameter were purchased from Sigma Life Science and 12 nm gold nanoparticles (capped with citrate) were obtained from NanoComposix (San Diego, CA). Sodium dodecyl sulfate (SDS), 3-aminopropyltriethoxysilane (APTES), 25% glutaraldehyde, cetyl-tri-methylammonium bromide (CTAB), and Triton X-100 were purchased from Sigma-Aldrich. Stretavidin-Cy5 was purchased from GE Healthcare. Saline sodium citrate (SSC) 1X buffer was made by mixing 15 mM sodium citrate with 150 mM sodium chloride. Negative photoresist (SU-8 50) and its developer were purchased from MicroChem Corp. (Newton, MA). Circular glass chips with 4 in. diameter and a 0.6 in. center hole were obtained from Precision Glass & Optics (Santa Ana, CA, USA).

All reagents and materials required for SPR experiments, including 1-ethyl-3-(3-dimethylaminopropyl) carbodiimide (EDC), N-hydroxysuccinimide (NHS), ethanolamine, HBS-N Buffer (0.01 M HEPES pH 7.4, 0.15 M NaCl), and CM5 sensor chips, were purchased from GE Healthcare (UK).

All oligonucleotides (listed in Table S1 in the ESM) were synthesized and modified by Integrated DNA Technologies (Coralville, IA). Target oligonucleotides (20- or 60-mer) representing different SNPs of *KRAS* gene codon 12 (G12A (A) and wild-type (W)) as well as 20-mer B and NB targets (fungal pathogenic sequences [22]) were modified with a biotin molecule at the 5′ end. The sequences were designed in such a way that the SNP sites were located at the center of the oligonucleotides. The 20-mer probe oligonucleotides were modified with an amine group and a C12 spacer at the 5′ end.

Genomic DNA samples, containing different allele compositions of the *KRAS* gene codon 12 were obtained from QIMR Berghofer Medical Research Institute (Brisbane, Australia). In order to obtain the 80 bp PCR products, a pair of forward and reverse primers (Table S1 in the ESM) was used. A custom PCR protocol on a thermocycler (Cetus, Perkin Elmer) was used for DNA amplification. Thermocycling was initiated by 3 minutes of denaturation, followed by 30 thermal cycles at 95 ˚C for 40 s (denaturation), 55 ˚C for 30 s (annealing) and 72 ˚C for 60 s (extension), and terminated by 10 minutes of final extension at 72 ˚C. The amplified products were purified using a nucleotide removal kit from Qiagen Inc. (Toronto, ON, Canada).

### 2.2 DNA hybridization on a CD-NBA chip

The CD-NBA chip is comprised of a PDMS slab (4 in. in diameter) with 96 radial microchannels, sealed reversibly to a circular glass chip. The width of straight radially arranged channels was 200 μm and the height was 35 μm. The probe immobilization procedure was similar to previously reported methods [23, 24]. Briefly, 0.5 μL of probe solution (in 1.0 M NaCl + 0.15 M $NaHCO_3$) was added to the inlet reservoirs of the CD-NBA chip, which was then placed on a rotating platform. The solutions were introduced into the radial channels by spinning the circular chip at 400 rpm for 3 min. The probe solutions were driven out from the channel after 20 min of incubation at room temperature by spinning the chip at 1,800 rpm for 1 min. Subsequently, the radial PDMS slab was peeled off, leaving behind 96 radial probe lines printed on the glass chip, which was then rinsed and dried. Subsequently, another PDMS slab with 96 spiral channels was sealed against the glass chip pre-printed with the probe lines for carrying out the DNA hybridization. The width of spiral channels was 100 μm and the height was 35 μm. The target solution (1 μL), prepared in hybridization buffer (1X SSC + 0.2% SDS) with a final concentration of 10 nM, was added to the inlet reservoir and then flowed into the spiral channel using a spin rate of 900 rpm. This spin rate resulted in approximately 13 min of dynamic hybridization of the targets to the complementary probes at the intersections of spiral channels with the radially arrayed probe lines. High-temperature experiments were achieved by heating the CD-NBA chip using a hot air blower. The temperature was calibrated in a separate experiment using a temperature sensor placed on the glass chip surface, sealed with the PDMS slab on the surface.

The washing procedure was performed after DNA hybridization. The wash solution was SSC with NaCl concentrations ranging from 10 to 300 mM. The washing buffer contained either no AuNPs or AuNPs of various concentrations from 0.2 to 40 nM. In order to stabilize the AuNPs against salt aggregation, they were loaded with DNA oligonucleotides, with sequences irrelevant to the target strands, prior to addition to the wash buffer. This was performed by mixing various concentrations of 12- or 20-mer oligonucleotide with AuNPs and incubating the mix at 95 ˚C for 5 min. Subsequently, 2 μL of the AuNP wash buffer was added to the inlet reservoirs of the spiral channels. A dynamic wash was performed by spinning the CD-NBA chip at spin rates of 700 to 1,500 rpm. Stop-flow wash was performed by spinning the chip at 2,200 rpm for 20 s in order to fill the channels with the wash buffer, incubating for 15 min (stop-flow), and then ejecting the buffer with a spin at 2,200 rpm for another 20 s. After washing (dynamic or stop-flow) was completed, streptavidin-Cy5 solution (50 μg/mL in 1X PBS buffer) was added to the inlet reservoir and allowed to flow into the channel by spinning at 1,500 rpm. Finally, the spiral PDMS slab was peeled off from the glass chip.

Fluorescence detection was conducted by scanning the glass chip on a confocal laser fluorescence scanner (Typhoon 9410, GE Healthcare) at 10 μm resolution, as previously described [23, 24]. The excitation and emission wavelengths were 633 and 670 nm, respectively. The photomultiplier tube voltage was set at 600 V. The scanned image was analyzed using the IMAGEQUANT 5.2 software.

### 2.3 DNA adsorption on AuNPs

In order to study the kinetics of adsorption of DNA oligonucleotides on the surface of AuNPs, fluorescence quenching was measured. Cy5-labeled W20 oligonucleotides (8 nM) were prepared in 1 mL of sodium citrate buffer (15 mM) in a polystyrene cuvette. The buffer contained NaCl concentrations of 0, 10, 30, 50, 70, 90, 110, 130, and 150 mM. The cuvette was placed in the holder of a spectrofluorometer (Photon Technology International). Then, 1 mL of aqueous AuNP colloid (80 nM) was added to the cuvette and the contents were mixed. Immediately after, the fluorescence intensity (excitation at 650 nm and emission at 670 nm) was monitored for 7 min using the time-based mode.

### 2.4 Surface plasmon resonance (SPR) spectroscopy

SPR measurements were performed on BIAcore X100 (GE Healthcare) as previously described [21]. Briefly, immobilization of the amine-labeled 20-mer probes (A) was performed on the surface of a sensor chip (CM5), using a company-developed method [21, 25]. The carboxylic groups on the sensor surface were activated by an EDC/NHS mixture (1:1 *v*/*v*). Then, the amine-labeled probe molecules were immobilized on the sensor surface by running the immobilization solution containing the probe molecules (50 μM) and CTAB (0.6 mM) over the sensor surface. Finally, unreacted succinimide groups were deactivated using an ethanolamine solution (pH 8.5). The target solutions were prepared in HBS-N buffer with DNA target concentrations of 10, 20, 40, 80, and 160 nM. The rate constants of DNA hybridization and dehybridization were determined using the multi-cycle kinetic procedure. Briefly, 10 nM target solutions continuously flowed over the sensor chip surface (with immobilized probe) for 60 s. After hybridization, washing was achieved by a continuous flow of wash buffer over the sensor surface for 240 s. In the stringent wash experiment, the HBS-N buffer was used as the wash buffer. However, the AuNP wash buffer contained 5 nm AuNPs (10 nM) in the HBS-N buffer. The nanoparticles in the AuNP wash buffer had been previously loaded with the 20-mer oligonucleotides (stabilizers with a sequence unrelated to the target and probe), by mixing the stabilizers with AuNPs in water and then incubating the mix at 95 °C for 5 min. After each hybridization-wash cycle, the sensor surface was regenerated (all the target strands were washed away) by running an alkaline wash (50 mM NaOH) for 30 s. This cycle of hybridization, wash, and regeneration was repeated for the other 4 target concentrations of 20, 40, 80, and 160 nM.

## 3 Results and discussion

For nucleic acid analyses, we previously developed a CD-like chip for microfluidic DNA hybridization that provided the advantage of fast analysis and multiplex capability [23, 24]. This platform, termed as CD-like NanoBioArray chip or CD-NBA chip, utilizes centrifugal force to flow the target solutions within the microfluidic channels. As shown in Fig. 1, the target molecules hybridize to their complementary probes located at the intersections of the spiral channels to the radially patterned probe lines. These probe lines have previously been printed on the surface of the chip, and hybridization occurs between the target DNA molecules (biotin-labeled for post-hybridization fluorescence labeling) and complementary DNA probes, giving rise to fluorescence hybridization patches. Figure 2(a) shows the fluorescence image of the hybridization on a region of the CD-NBA chip, in which several spiral channels intersect with four probe lines. After DNA hybridization, different types

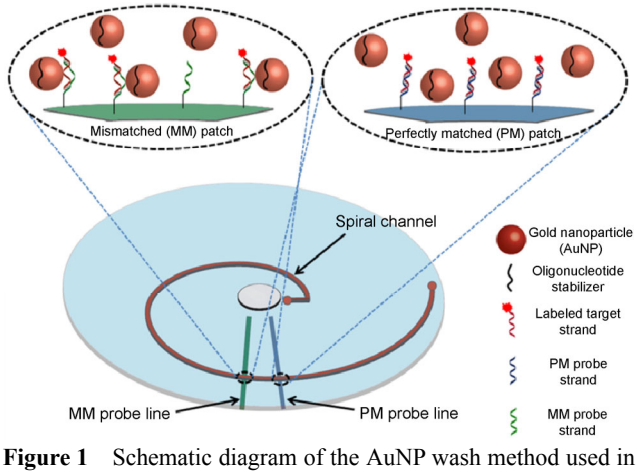


**Figure 1** Schematic diagram of the AuNP wash method used in CD-NBA chip, with one of the many spiral channels shown. The inset shows destabilization by AuNPs at mismatched, but not perfectly matched, hybridization patches. The chip diagram is not drawn to scale.

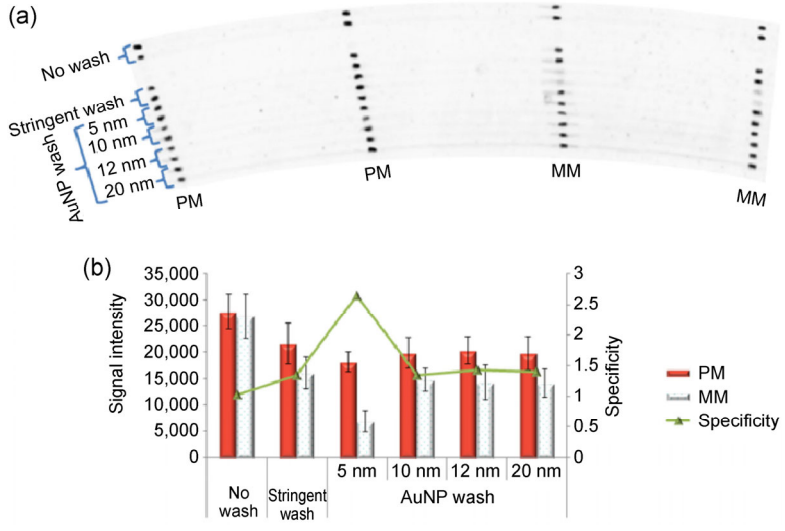


**Figure 2** (a) Fluorescence image of a part of the CD-NBA chip showing the hybridization patches obtained from 12 spiral channels. These patches (200 μm × 100 μm) were obtained from the hybridization of 1 μL of A20 targets (10 nM) in the spiral channels with their corresponding PM and MM probes (A and W, respectively) pre-printed in a radial fashion on the chip. The hybridization step was performed at 22 °C with a spin rate of 900 rpm. The hybridization patches were either not washed ("no wash"), washed with 2 μL of the hybridization buffer ("stringent wash") or washed with the hybridization buffer containing AuNPs of different sizes (5, 10, 12, 20 nm diameter) ("AuNP wash"). The wash buffer was introduced in the spiral channel using a spin rate of 900 rpm (see Fig. S2 in the ESM for an investigation on the effect of flow-mediated dynamic wash). Oligonucleotides of irrelevant sequences (10 nM, 20-mer) were loaded on the surfaces of nanoparticles to stabilize them against salt-induced aggregation. (b) The histogram shows the signal intensities of the hybridization patches obtained along the spiral target channels, with the specific signals (on PM probe lines) represented by blue hatched bars and nonspecific signals represented by red solid bars. The error bars show the standard deviations of 8 measurements. The green line shows the specificity, which is determined by dividing the intensity of the PM spots by that of the MM patches (see Fig. 1).

of washes were applied to the spiral channels. The histogram of the fluorescence intensities of the patches is shown in Fig. 2(b), with the specificity ($\sigma$) shown in Eq. (1) as follows

$$\sigma = \frac{S_{PM}}{S_{MM}} \quad (1)$$

where $S_{PM}$ and $S_{MM}$ represent the signal intensity at the PM and MM probe patches, respectively.

In DNA microarrays, the nonspecific signals are inevitably detected and they are conventionally reduced by conducting a stringent wash subsequent to DNA hybridization. To compare the methods of AuNP wash and stringent wash, the hybridization buffer (1X SSC) was allowed to flow into the spiral channels at room temperature, with or without AuNPs, respectively. The stringent wash resulted in a specificity of 1.3 (compared to 1 in "no wash" channels). However, the use of AuNPs in the wash step helped to increase the specificity to 2.6. This was observed only in the presence of 5 nm AuNPs, not with 10, 12, or 20 nm. This result is in agreement with the previous observation of the AuNP-conjugated DNA targets that small nanoparticles (5 nm diameter), but not the larger 12 nm nanoparticles, enhance the DNA dehybridization rates [21]. We attribute the success of using 5 nm AuNPs to their high degree of curvature, which reduces the Columbic repulsion between AuNP surfaces and the double-stranded segments of the duplexes [21].

### 3.1 Signal/specificity correlation in the AuNP wash technique

In the stringent wash method, high-temperature and/or low-salt conditions are used to create a destabilizing environment for the formed duplexes and accelerate their dehybridization. This method aims to remove the nonspecific duplexes more than their specific counterparts, thus enhancing the specificity. We compared the AuNP wash to the stringent wash methods directly. Figures 3(a) and 3(b) show the histograms

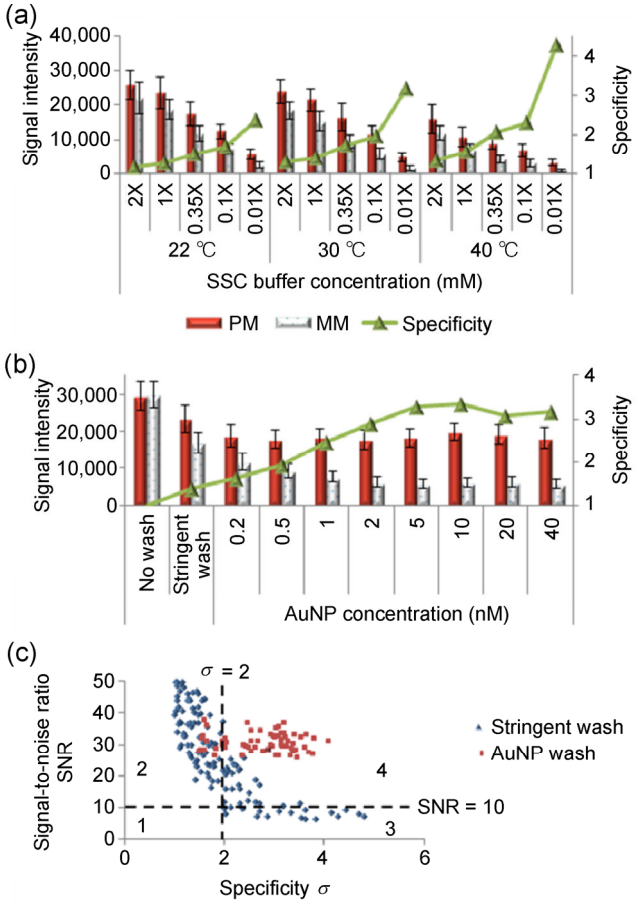


**Figure 3** Comparison of the stringent wash and AuNP wash methods in terms of sensitivity and specificity. (a) The histogram shows the hybridization signals in fluorescence units obtained after the stringent wash. After DNA hybridization of A20 targets with their PM probes (A) and MM probes (W), the hybridization patches were washed with 2 μL of SSC buffer with concentrations from 0.01X to 2X (i.e., NaCl concentrations from 1.5 to 300 mM, respectively) at 3 different temperatures of 22, 30, and 40 ˚C. For details, see Fig. S3 in the ESM. (b) Histogram shows the hybridization signals obtained after the AuNP wash. The 1X SSC buffer solution (consisting of 150 mM of NaCl) contained 5 nm AuNPs with various concentrations from 0.2–40 nM. Error bars in (a) and (b) show the standard deviations of 10 measurements. For other conditions, see Fig. 2. (c) The plot shows the correlation between the signal-to-noise ratio (SNR) of the PM spots with their specificities ($\sigma$) for stringent wash (blue data points) and AuNP wash (red data points). The data were obtained from measurements using 4 different CD-NBA chips. The SNR values are the ratios of PM signal intensities over the average noise (~480 fluorescence units). A SNR of 10 was chosen as the minimum acceptable value. The typical values of standard deviations of the hybridization signals at a SNR of 10 were used to calculate the corresponding minimum acceptable value for $\sigma$ at the 95% confidence level ($\sigma \approx 2$). The plot area was divided into 4 regions showing low $\sigma$/low SNR (region 1), low $\sigma$/high SNR (region 2), high $\sigma$/low SNR (region 3), and high $\sigma$/high SNR (region 4).

resulting from the hybridization signals obtained by the stringent and AuNP wash techniques, respectively. Figure 3(a) demonstrates that the specificity increases as the level of stringency increases (i.e., higher temperature and less salt). However, the PM signal decreases simultaneously, resulting in a negative correlation (anticorrelation) between the signal and specificity. We applied the Pearson correlation coefficient ($r$) as a measure of correlation of the PM signal ($S_{PM}$) and specificity, see Eq. (2) as follows [26]

$$r = \frac{\Sigma_{i=1}^{n}(S_{PM}^{i} - \bar{S}_{PM})(\sigma^{i} - \bar{\sigma})}{\sqrt{\Sigma_{i=1}^{n}(S_{PM}^{i} - \bar{S}_{PM})^{2}}\sqrt{\Sigma_{i=1}^{n}(\sigma^{i} - \bar{\sigma})^{2}}} \quad (2)$$

where $S_{PM}$ represents the PM signal intensity at different washing conditions; $\bar{S}_{PM}$ is the average intensity for PM signals; $\sigma^{i}$ is the specificity (calculated by Eq. (1)) at each washing condition; $\bar{\sigma}$ is the average specificity; $n$ is the number of data points.

While $r = 0$ represents no correlation, $r = -1$ shows the highest anticorrelation between the signal and specificity. From the signals and specificities shown in Fig. 3(a), the $r$ value is determined to be −0.92, which indicates a strong anticorrelation between the two parameters. Unfortunately, this anticorrelation between signal and specificity is frequently reported in DNA hybridization experiments using the stringent wash method [11, 12, 27], and high specificity appears to only be achieved at the expense of the signal [11]. In contrast, washing of the duplexes using buffer solutions carrying AuNPs does not result in such a strong anticorrelation. Figure 3(b) shows the hybridization signals after washing the duplexes with hybridization buffers containing AuNPs at various concentrations. The MM signals decrease as the AuNP concentrations increase from 0.2 to 5 nM but no further decrease is observed at higher AuNP concentrations (5–40 nM). Since the PM signals are not reduced with increasing AuNP concentration, this leads to a maximum specificity of 3.2 at 5 nM AuNP. The calculated $r$ value for the AuNP wash method is −0.16, which indicates a much lower signal/specificity anticorrelation, or almost no correlation, compared to the value of −0.92 obtained from the high-temperature/low-salt stringent wash method.

The difference between the $r$ values obtained from the AuNP and stringent washes is also illustrated in our

analysis of approximately 400 hybridization patches obtained by both methods. Figure 3(c) shows a plot of SNR vs. $\sigma$ obtained from AuNP and stringent washes. We defined the minimum acceptable values for SNR as 10 and $\sigma$ as 2. We also divided the plot into 4 regions of low $\sigma$/low SNR (region 1), low $\sigma$/high SNR (region 2), high $\sigma$/low SNR (region 3), and high $\sigma$/high SNR (region 4). As expected, the majority of the data points resulting from the stringent wash are distributed in regions 1–3. Interestingly, the data points from the AuNP wash method are primarily localized in region 4, which corresponds to the desirable outcome of high $\sigma$ and SNR.

The outcome of high $\sigma$ and minimal loss in SNR observed with the AuNP wash method can be explained in terms of the dehybridization rate constant $k_d$, which is experimentally determined from our kinetic analyses using SPR spectroscopy. For the MM duplex, the $k_d$ value increased by five folds from $3.2 \times 10^{-4}$ s$^{-1}$ for the stringent wash to $15.9 \times 10^{-4}$ s$^{-1}$ for AuNP wash at 22 ˚C (Table 1). Conversely, the $k_d$ value for the PM duplex demonstrated only a slight increase from $1.7 \times 10^{-4}$ s$^{-1}$ for the stringent wash to $3.0 \times 10^{-4}$ s$^{-1}$ for the AuNP wash. This increase in $k_d$ value for the AuNP wash (less than two fold) is much smaller than the corresponding increase at 40 ˚C for the stringent wash (five-fold). The latter is attributed to the enhanced destabilization of the MM duplexes by AuNPs. However, increasing the stringent wash temperature from 22 to 40 ˚C enhanced the $k_d$ values of both MM and PM duplexes, demonstrating the undesirable destabilization of PM duplexes, and the desirable destabilization of MM duplexes. These observations explain our previous findings using the CD-NBA chip, that the PM signals are only slightly affected compared to their MM counterparts using the AuNP wash method, leading to preservation of the signal.

**Table 1** Dehybridization rate constants of PM and MM duplexes using stringent wash vs. AuNP wash, as determined by SPR spectroscopy (Fig. S4 in the ESM)

| | | Stringent wash | | AuNP wash |
|---|---|---|---|---|
| | | 22 ˚C | 40 ˚C | 22 ˚C |
| $k_d$ ($10^{-4}$ s$^{-1}$) | PM | 1.7 (±0.3)[a] | 8.1 (±0.8) | 3.0 (±0.7) |
| | MM | 3.2 (±0.7) | 18.7 (±0.9) | 15.9 (±1.3) |

[a]All standard errors are determined from two measurements each including five different target concentrations of 10, 20, 40, 80, and 160 nM.

We attribute the difference in enhanced destabilization of the MM duplexes, observed for the AuNP wash compared to the stringent wash, to the specific mechanism on which the AuNP wash technique is based. During dehybridization, AuNPs bind to ssDNA segments (bubbles) [21], which are constantly formed by a phenomenon called thermal breathing [28]. The presence of a mismatch base pair, through a cooperative effect, causes weakening and disruption of the neighboring base pairs, resulting in the formation of more bubbles [29]. In 2006, Zeng et al. compared the dissociation curves obtained from PM and MM duplexes, and found that the amount of bubbles was drastically enhanced in the presence of a single MM site in the middle of the duplex [30]. The greater amount of bubbles in the MM duplexes makes them susceptible to binding by AuNPs, leading to the success of the AuNP wash method. The AuNP wash method targets the bubbles in MM duplexes for their accelerated dehybridization or destabilization, to a much larger extent than in the case of PM duplexes. This mechanism of destabilization of MM duplexes causes an enhancement in specificity without reducing the signal, leading to the observed low negative $r$ value or virtually no anticorrelation between signal and specificity. In contrast, the stringent wash method has similar destabilizing influences on the PM and MM duplexes, which lead to similar accelerated dehybridization effects and the observed high signal/specificity anticorrelation or high negative $r$ value.

The preserved sensitivity with improved specificity is an exclusive feature of the AuNP wash method. This feature was not achieved in the previous AuNP-enabled method, in which AuNP was used in the hybridization step but not in the wash step [19]. In the previous method, the hybridization signals obtained from DNA targets that are conjugated to AuNPs (AuNP targets) were observed to be lower than the signals from free targets. This was attributed to the low hybridization rate constants ($k_h$) of DNA targets conjugated to AuNPs [21]. This experiment has been repeated using the CD-NBA chip and shown in Fig. S1 in the ESM.

### 3.2 Optimization of the AuNP wash method

In order to optimize the AuNP wash method, we evaluated the effect of different experimental factors including the salt content of the buffer medium, and the length and concentration of the oligonucleotide stabilizer (used to prevent AuNPs in the wash buffer from forming aggregates) on the performance of the method. We hypothesized that optimization of these factors could improve the effectiveness of AuNP destabilization of MM duplexes, and thus the efficacy of the method.

The histogram in Fig. 4(a) shows the hybridization signals after stringent wash. As the salt concentration is reduced, the signal decreases, and the specificity increases. This signal/specificity anticorrelation is consistent with the results in Fig. 3(a), which displayed data at narrower range of salt concentrations, albeit at several temperatures. The histogram in Fig. 4(b) shows the hybridization signals after washing with buffer solutions containing 5 nM of AuNPs (5 nm AuNP, 150 mM NaCl). Figure 4(b) displays a similar increase in specificity with reduced salt concentration from 150 to 90 mM. However, at lower salt concentrations (from 50 to 10 mM of NaCl) a decrease in specificity was observed, reaching values that were comparable to the values obtained from the stringent wash method. This indicates that the AuNPs become ineffective at destabilizing MM duplexes at low salt concentrations. We attribute this ineffectiveness to the low extent of binding between AuNP surfaces and the ssDNA segments of the duplexes (bubbles) at low salt concentrations. To demonstrate this low rate of binding, we measured the adsorption kinetics of ssDNAs onto the surfaces of AuNPs at different salt concentrations. This measurement is based on the fact that the emission of the fluorescently labeled DNAs is quenched after binding to AuNPs. Figure 4(c) shows the kinetic traces of the normalized fluorescence of a fluorescently labeled 20-mer oligonucleotide upon mixing with AuNPs at different NaCl concentrations. The pseudo first-order rate constant of adsorption of oligonucleotides onto the AuNP surfaces, $k'_a$, was obtained from the exponential fit of the kinetic data (Fig. 4(c)). The $k'_a$ value increased from $1.64 \times 10^{-4}$ $s^{-1}$ at the no-salt condition to $490 \times 10^{-4}$ $s^{-1}$ at 150 mM of salt. This increase

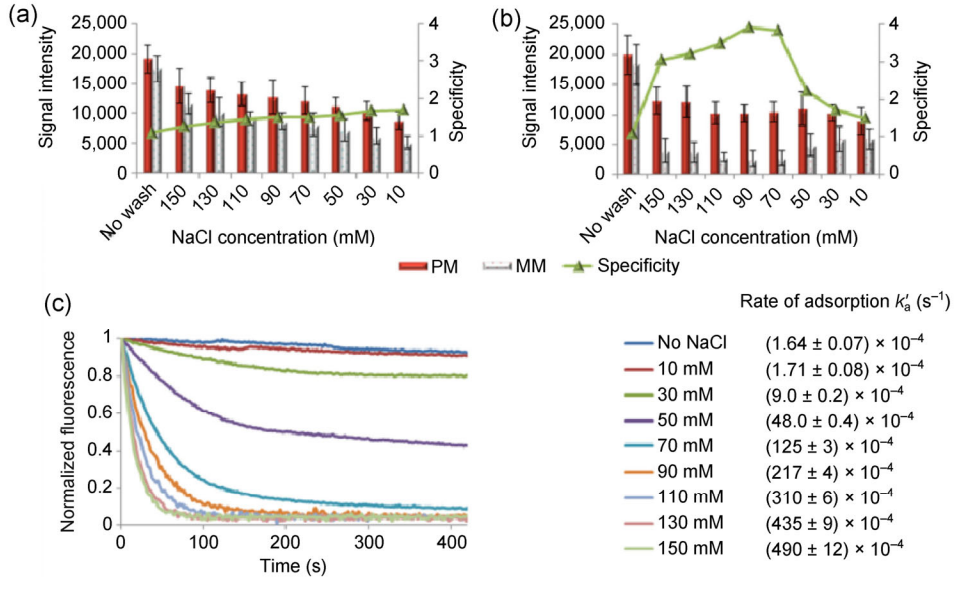


**Figure 4** Optimization of the salt content used in the AuNP wash method. Histograms of hybridization signals obtained from washing of the hybridization patches using wash buffers containing different concentrations of NaCl (10–150 mM) at 22 °C. The buffer solutions either contain (a) no AuNPs or (b) AuNP (5 nm) with a concentration of 5 nM. For other conditions see Fig. 2. (c) Kinetics of the adsorption of Cy5-labeled 20-mer oligonucleotides C-W20 onto 5 nm AuNPs in sodium citrate buffer (15 mM) at different NaCl concentrations ranging from 0 to 150 mM. Each curve represents the normalized fluorescence by expressing the time-dependent fluorescence intensity as a fraction of the initial intensity. The rate of adsorption, $k'_a$, at each NaCl concentration, as obtained from the exponential fit of the normalized data, is shown beside the legend of the corresponding curve.

in $k'_a$ value with high salt concentrations can be explained by the fact that electrostatic repulsion between the negatively charged DNA backbone and the citrate-capped surfaces of AuNPs is reduced by charge screening at high salt concentrations [31].

The results in Fig. 4(c) could explain the salt-dependency of AuNP-destabilization, and the specificities observed in Fig. 4(b). First, an increase in the salt content enhances AuNP–ssDNA binding, due to the charge screening effect on AuNPs and ssDNAs. This effect enhances the effectiveness of the AuNP wash method, and thus the specificity. The sharp enhancement in specificity resulting from performing the AuNP wash method at salt concentrations of 30 to 70 mM (Fig. 4(b)) indicates that the charge screening of AuNP–ssDNA prevails at this salt concentration range. Second, salt also decreases specificity through charge screening of probe ssDNAs and target ssDNAs. This phenomenon is similarly observed in both the AuNP (Fig. 4(b)) and stringent wash techniques (Figs. 3(a) and 4(a)). The decrease in specificity at high salt concentrations (90 to 150 mM NaCl) shows that, at this range of salt content, the increase in the AuNP–ssDNA binding is less effective than the increase in probe-target binding.

In order to stabilize AuNPs in the wash buffer and prevent salt-induced aggregation, the AuNP surfaces were loaded with oligonucleotide stabilizers with sequences non-complementary to the probe/target sequences. Here, we investigated the effects of length and concentration of the oligonucleotide stabilizers on the specificities obtained using the AuNP wash method. Figure 5(a) shows the hybridization signals after the duplexes were washed with solutions containing AuNPs that were stabilized with 12-mer and 20-mer of irrelevant oligonucleotides of different concentrations. We observed that higher specificities were obtained when shorter oligonucleotides (12-mer rather than 20-mer) or lower concentrations of oligonucleotide were used. The increased specificity observed could be due to the fact that oligonucleotide stabilizers with shorter sequence lengths and lower concentrations occupy smaller portions of the AuNP surfaces, thus leaving more surfaces available for binding to the ssDNA segments of the duplexes. Additionally, since the negative charges of the oligonucleotides add to the negative charge density of the AuNP surfaces and hinder AuNPs from approaching and attaching to the negatively-charged duplexes, shorter lengths and lower concentrations of the oligonucleotide stabilizer will lead to improved effectiveness in AuNP-induced destabilization of MM duplexes, and increased specificity.

### 3.3 Application to genomic samples

In order to investigate the applicability of the AuNP wash technique for genomic samples, we first evaluated the robustness of the technique upon sequence variation (i.e., the purine content), and then evaluated the

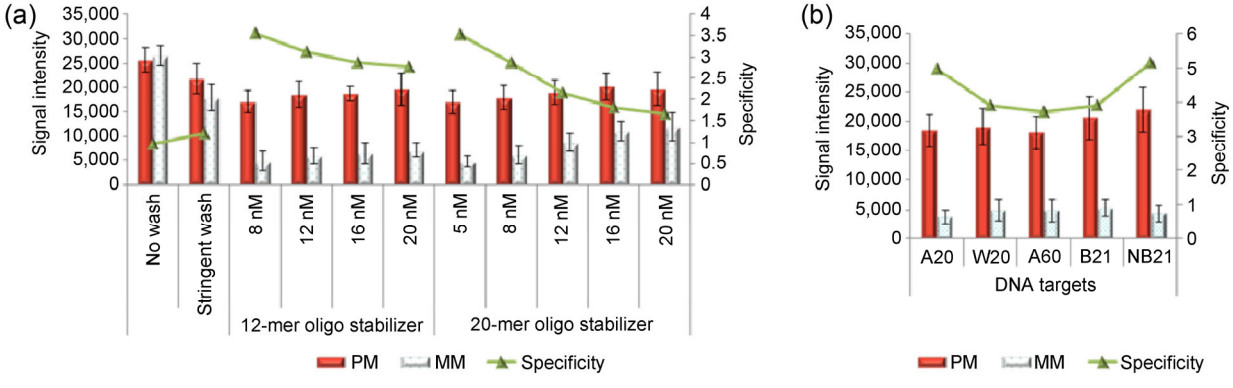


**Figure 5** Optimization of various experimental factors such as oligonucleotide stabilizer and purine content of DNA targets in the AuNP wash method. (a) Histogram of the hybridization signals obtained after washing with SSC buffer solution (with 90 mM NaCl) containing AuNPs stabilized with different oligonucleotides. The 5 nm AuNPs (5 nM) were first stabilized with 12-mer and 20-mer oligonucleotides of different concentrations (8–20 nM for 12-mer and 5–20 nM for 20-mer). (b) Histogram of the fluorescence intensity obtained at the hybridization patches of various targets following AuNP wash using SCC buffer (with 90 mM NaCl) containing 5 nm AuNPs (5 nM) first stabilized with 12-mer oligonucleotides of 8 nM. For other conditions see Fig. 2.

performance of the technique using PCR amplicons as the target strands.

In order to evaluate the robustness of the AuNP wash technique, we employed three sequences related to the *KRAS* gene (A20, A60, and W20), and two sequences related to a fungal pathogen (B21, NB21) (Table S1 in the ESM). In W20 and A60 targets, the 20 bases of the target that hybridize with the probes are similar to A20 except for variations in the type of the mismatch base pair (C–C base pair in A20 and A60 vs. G–G in W20) and also in the length of the target (60 bases in A60 vs. 20 bases in A20). These sequence variations do not affect the performance of the technique (Fig. 5(b)). Experiments were also performed using sequences that are completely different from A20, i.e., B21 and NB21. The strength of binding with gold is known to vary among DNA bases, and purine bases (A and G) are known to bind more strongly with the gold surface than pyrimidine bases (C and T) [32]. Since B21 and NB21 targets have lower purine base contents in their sequences than the A20 target (approximately 40% in B21/NB21 targets vs. 60% in A20), we expect to observe lower specificities with the B21 and NB21 targets. However, the lower purine base content of B21/NB21 targets did not result in a decrease in specificity (Fig. 5(b)). Since binding of AuNPs to either the target strand or the probe strand can accelerate the dehybridization process, the weaker binding between AuNPs and the pyrimidine-rich strand offset the stronger binding between AuNPs and the complementary purine-rich strand. This offset effect leads to an insensitivity of the AuNP wash method to the purine content of the DNA sequence. With the robustness of the method demonstrated, we conclude that the AuNP wash method can be applied to hybridization experiments involving DNA strands with various sequences.

We have also used the AuNP wash method to detect SNPs in genomic samples, which consist of 4 different alleles of the *KRAS* gene codon 12. Detection of these SNPs is critical for clinicians to choose the appropriate type of therapy for colorectal cancer patients [33]. Figure 6(a) shows the fluorescence image of the signals obtained from PCR amplicons that have been hybridized to the probes on the surface of the CD-NBA chip followed by AuNP wash. As displayed in Fig. 6(b), the specificity was enhanced without compromising the signal, leading to a sensitive and specific SNP discrimination obtained at ambient temperature (22 ˚C). These results, obtained using AuNPs

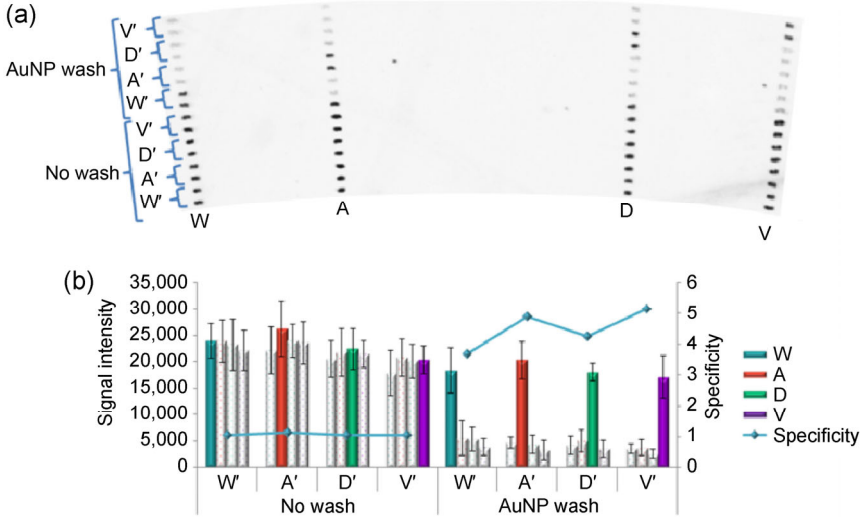


**Figure 6** Hybridization of PCR amplicons, with their corresponding PM and MM probes in the CD-NBA chip. (a) Scanned fluorescence image and (b) histogram. The target molecules (80 base pairs) were amplified from 4 different alleles of *KRAS* gene codon 12 and hybridized with their complementary probes preprinted on the chip surface. Each probe is perfectly matched with one of the targets and single base-pair mismatch with the other 3 targets. After hybridization, washing was conducted with a flow of wash buffer (SSC buffer with 90 mM NaCl) containing 5 nm AuNPs (5 nM, stabilized with 8 nM of 12-mer oligonucleotides) at a temperature of 22 ˚C and a spin rate of 900 rpm.

in the wash solution, are in sharp contrast to the previous results in Fig. S1 (see ESM) obtained using AuNPs conjugated to the DNA targets in the hybridization solution. This is because the sensitivity of the PM duplexes in the current AuNP wash method is preserved while the specificity is enhanced.

## 4 Conclusions

We have developed a technique for enhancing the specificity of DNA hybridization without reducing the signal. This technique is called the AuNP wash technique, and is performed on a CD-NBA chip using a buffer solution containing 5 nm gold nanoparticles. The solution dynamically washes the duplexes on the surfaces of the spiral channel of the chip and destabilizes the MM duplexes but not the PM duplexes. The nanoparticle does not bind to the fully coiled duplex, but targets only the ssDNA segments (bubbles) of the duplex in the course of dehybridization and accelerates the propagation of the bubbles as well as unzipping of the duplex. This mechanism of destabilization causes a preferential removal of the MM duplexes, rather than the PM ones, and hence the signal is preserved, while the specificity is enhanced. We also investigated the influence of several governing factors of the method, and evaluated the performance of the technique with varying DNA sequences. The method was applied to the detection of *KRAS* gene SNP variations in genomic samples. Furthermore, SNP discrimination is achieved at a single temperature, alleviating the difficulty of temperature optimization for multiple targets of different melting temperatures in multiplex analysis. In contrast to the other attempts (e.g., molecular beacons) to enhance the specificities of DNA hybridization, no complicated design for the DNA probe sequence is required and high specificity is effectively achieved via a simple wash step subsequent to DNA hybridization. This simplicity is an advantage that, together with the robustness of sequence variation and compatibility with multiplex analyses, makes this technique a promising tool to be used in DNA hybridization-based microarrays. Additionally, it has the potential to reduce false positive/negative results and improve the accuracy of the microarray results.

## Acknowledgements

We gratefully acknowledge financial support from a Discovery Grant of Natural Sciences and Engineering Research Council of Canada (No. NSERC216925), Dr. Dipankar Sen for useful advice and technical support as well as Dr Naveed Gulzar for his assistance in the SPR measurements.

**Electronic Supplementary Material**: Supplementary material (the sequences of probe, target and primer oligonucleotides, the results of SNP detection of AuNP-loaded PCR products, the fluorescence image of hybridization signals after dynamic wash and stop-flow wash, after stringent wash and AuNP wash and the SPR sensograms resulted from kinetic analysis of DNA hybridization) is available in the online version of this article at http://dx.doi.org/10.1007/s12274-015-0893-9.

## References

[1] Gubala, V.; Harris, L. F.; Ricco, A. J.; Tan, M. X.; Williams, D. E. Point of care diagnostics: Status and future. *Anal. Chem.* **2012**, *84*, 487–515.

[2] Niemz, A.; Ferguson, T. M.; Boyle, D. S. Point-of-care nucleic acid testing for infectious diseases. *Trends Biotechnol.* **2011**, *29*, 240–250.

[3] Knez, K.; Spasic, D.; Janssen, K. P. F.; Lammertyn, J. Emerging technologies for hybridization based single nucleotide polymorphism detection. *Analyst* **2014**, *139*, 353–370.

[4] Koltai, H.; Weingarten-Baror, C. Specificity of DNA microarray hybridization: Characterization, effectors and approaches for data correction. *Nucleic Acids Res.* **2008**, *36*, 2395–2405.

[5] Chagovetz, A.; Blair, S. Real-time DNA microarrays: Reality check. *Biochem. Soc. Trans.* **2009**, *37*, 471–475.

[6] Wittwer, C. T. High-resolution DNA melting analysis: Advancements and limitations. *Hum. Mutat.* **2009**, *30*, 857–859.

[7] Urakawa, H.; El Fantroussi, S.; Smidt, H.; Smoot, J. C.; Tribou, E. H.; Kelly, J. J.; Noble, P. A.; Stahl, D. A. Optimization of single-base-pair mismatch discrimination in oligonucleotide microarrays. *Appl. Environ. Microbiol.* **2003**, *69*, 2848–2856.

[8] Marcelino, L. A.; Backman, V.; Donaldson, A.; Steadman, C.; Thompson, J. R.; Preheim, S. P.; Lien, C.; Lim, E.;

Veneziano, D.; Polz, M. F. Accurately quantifying low-abundant targets amid similar sequences by revealing hidden correlations in oligonucleotide microarray data. *Proc. Natl. Acad. Sci. USA* **2006**, *103*, 13629–13634.

[9] Rule, R. A.; Pozhitkov, A. E.; Noble, P. A. Use of hidden correlations in short oligonucleotide array data are insufficient for accurate quantification of nucleic acid targets in complex target mixtures. *J. Microbiol. Methods* **2009**, *76*, 188–195.

[10] Michiels, S.; Koscielny, S.; Hill, C. Prediction of cancer outcome with microarrays: A multiple random validation strategy. *Lancet* **2005**, *365*, 488–492.

[11] Demidov, V. V.; Frank-Kamenetskii, M. D. Two sides of the coin: Affinity and specificity of nucleic acid interactions. *Trends Biochem. Sci.* **2004**, *29*, 62–71.

[12] Poulsen, L.; Søe, M. J.; Snakenborg, D.; Møller, L. B.; Dufva, M. Multi-stringency wash of partially hybridized 60-mer probes reveals that the stringency along the probe decreases with distance from the microarray surface. *Nucleic Acids Res.* [online] **2008**, *36*, e132. http://www.ncbi.nlm.nih.gov/pubmed/18805905 (accessed Sep 19, 2008).

[13] Grimes, J.; Gerasimova, Y. V.; Kolpashchikov, D. M. Real-time SNP analysis in secondary-structure-folded nucleic acids. *Angew. Chem.* **2010**, *122*, 9134–9137.

[14] Kolpashchikov, D. M. Binary malachite green aptamer for fluorescent detection of nucleic acids. *J. Am. Chem. Soc.* **2005**, *127*, 12442–12443.

[15] Kolpashchikov, D. M. A binary DNA probe for highly specific nucleic acid recognition. *J. Am. Chem. Soc.* **2006**, *128*, 10625–10628.

[16] Marras, S. A.; Kramer, F. R.; Tyagi, S. Efficiencies of fluorescence resonance energy transfer and contact-mediated quenching in oligonucleotide probes. *Nucleic Acids Res.* [online] **2002**, *30*, e122. http://www.ncbi.nlm.nih.gov/pmc/articles/PMC135848/ (accessed Nov 1, 2002).

[17] Tyagi, S.; Kramer, F. R. Molecular beacons: Probes that fluoresce upon hybridization. *Nat. Biotechnol.* **1996**, *14*, 303–308.

[18] Zhang, D. Y.; Chen, S. X.; Yin, P. Optimizing the specificity of nucleic acid hybridization. *Nat. Chem.* **2012**, *4*, 208–214.

[19] Sedighi, A.; Li, P. C. H. *Kras* gene codon 12 mutation detection enabled by gold nanoparticles conducted in a nanobioarray chip. *Anal. Biochem.* **2014**, *448*, 58–64.

[20] Wang, L.; Li, P. C. H. Gold nanoparticle-assisted single base-pair mismatch discrimination on a microfluidic microarray device. *Biomicrofluidics* **2010**, *4*, 032209.

[21] Sedighi, A.; Li, P. C. H.; Pekcevik, I. C.; Gates, B. D. A proposed mechanism of the influence of gold nanoparticles on DNA hybridization. *ACS Nano* **2014**, *8*, 6765–6777.

[22] Koch, C. A.; Li, P. C. H.; Utkhede, R. S. Evaluation of thin films of agarose on glass for hybridization of DNA to identify plant pathogens with microarray technology. *Anal. Biochem.* **2005**, *342*, 93–102.

[23] Wang, L.; Li, P. C. H. Optimization of a microfluidic microarray device for the fast discrimination of fungal pathogenic DNA. *Anal. Biochem.* **2010**, *400*, 282–288.

[24] Wang, L.; Li, P. C. H.; Yu, H.-Z.; Parameswaran, A. M. Fungal pathogenic nucleic acid detection achieved with a microfluidic microarray device. *Anal. Chim Acta* **2008**, *610*, 97–104.

[25] Löfås, S.; Mcwhirter, A. The art of immobilization for SPR sensors. In *Surface Plasmon Resonance Based Sensors*. Homola, J., Ed.; Springer: Berlin Heidelberg, 2006; pp 117–151.

[26] Lee Rodgers, J.; Nicewander, W. A. Thirteen ways to look at the correlation coefficient. *Am. Stat.* **1988**, *42*, 59–66.

[27] Lomakin, A.; Frank-Kamenetskii, M. D. A theoretical analysis of specificity of nucleic acid interactions with oligonucleotides and peptide nucleic acids (PNAs). *J. Mol. Biol.* **1998**, *276*, 57–70.

[28] Kearns, D. R.; James, T. L. NMR studies of conformational states and dynamics of DN. *Crit. Rev. Biochem. Mol. Biol.* **1984**, *15*, 237–290.

[29] Dauxois, T.; Peyrard, M.; Bishop, A. R. Entropy-driven DNA denaturation. *Phys. Rev. E* **1993**, *47*, R44–R47.

[30] Zeng, Y.; Zocchi, G. Mismatches and bubbles in DNA. *Biophys. J.* **2006**, *90*, 4522–4529.

[31] Zhang, X.; Servos, M. R.; Liu, J. Surface science of DNA adsorption onto citrate-capped gold nanoparticles. *Langmuir* **2012**, *28*, 3896–3902.

[32] Demers, L. M.; Östblom, M.; Zhang, H.; Jang, N. H.; Liedberg, B.; Mirkin, C. A. Thermal desorption behavior and binding properties of DNA bases and nucleosides on gold. *J. Am. Chem. Soc.* **2002**, *124*, 11248–11249.

[33] Parsons, B. L.; Myers, M. B. Personalized cancer treatment and the myth of *KRAS* wild-type colon tumors. *Discov. Med.* **2013**, *15*, 259–267.